Current Research in Food Science 9 (2024) 100851

Contents lists available at ScienceDirect

Current Research in Food Science

journal homepage: www.sciencedirect.com/journal/current-research-in-food-science

The effect of nerve cells on the intestinal barrier function and the influence of human milk oligosaccharides (hMOs) on the intestinal neuro-epithelial crosstalk

Xiaochen Chen [a,*], Naschla Gasaly [a,b], Xin Tang [a], Marthe T.C. Walvoort [c], Paul de Vos [a]

[a] Immunoendocrinology, Department of Pathology and Medical Biology, University Medical Center Groningen, University of Groningen, Groningen, the Netherlands
[b] Laboratory of Innate Immunity, Program of Immunology, Institute of Biomedical Sciences, Faculty of Medicine, Universidad de Chile, Santiago, Chile
[c] Stratingh Institute for Chemistry, Department of Chemical Biology, University of Groningen, Groningen, the Netherlands

ARTICLE INFO

Handling Editor: Yeonhwa Park

Keywords:
Enteric nervous system
Nerve cells
Gut barrier function
Transepithelial electrical resistance
Tight junction
2′-fucosyllactose (2′-FL)
3-fucosyllactose (3-FL)

ABSTRACT

The intestinal epithelium is an important gatekeeper of the human body by forming a barrier for the luminal content of the intestine. The barrier function is regulated by a complex crosstalk between different cell types, including cells from the enteric nervous system (ENS). ENS is considered to influence gastrointestinal processes and functions, but its direct effect on epithelial barrier function remains to be confirmed. To investigate the effect of nerve cells on the gut barrier function, an *in vitro* co-culture system was established in which T84 intestinal epithelial cells and SH-SY5Y nerve cells were seeded in ratios of 29:1 and 14:1. When the epithelial barrier was disrupted with the calcium ionophores A23187, we found that nerve cells exert a protective effect on A23187-induced disruption and that this protective effect is nerve cell concentration-dependent. This was demonstrated by rescuing effects on transepithelial electrical resistance (TEER) and upregulation of tight junction (TJ) protein expression. Furthermore, we studied whether similar rescuing effects could be achieved with the human milk oligosaccharides (hMOs) 2′-fucosyllactose (2′-FL) and 3-fucosyllactose (3-FL). Our results illustrate that in the presence of nerve cells 2′-FL and 3-FL do not have any additional rescuing effects, but that these hMOs can substitute the rescuing effects of nerve cells in the absence of nerve cells. Meanwhile, 2′-FL and 3-FL show different regulation effects on TJ expression. These findings provide valuable insights into potential therapeutic strategies for maintaining intestinal barrier integrity.

1. Introduction

The intestinal epithelium forms the main line of defense between the human body and the external environment (Chelakkot et al., 2018; Takiishi et al., 2017). The intestinal epithelial layer forms a barrier to prevent pathogens, toxins, and other undesired agents from entering the human body (Chen and de Vos, 2023; Gieryńska et al., 2022). Therefore, maintaining barrier integrity is crucial. Tight junctions (TJs) located in the apical part of the lateral membrane of intestinal epithelial cells play a key role (Ali et al., 2020; di Vito et al., 2022; Suzuki, 2020) in maintaining barrier integrity. TJs are assembled by a variety of proteins including transmembrane proteins such as claudin and occludin, and intracellular plaque proteins such as zonula occludens (ZO) (Suzuki, 2020). Claudins and occludins interacting with ZO connected to the actin cytoskeleton regulate the paracellular permeation of content from the lumen into the systemic circulation (Kaminsky et al., 2021; König et al., 2016). Therefore, a defective intestinal TJ barrier might result in leakage of harmful substances or pathogens to the circulation eventually leading to the development of intestinal inflammatory diseases (Kaminsky et al., 2021). The barrier is also tightly regulated by crosstalk with other intestinal components such as gut microbiota, and immune cells but also with the enteric nervous system (ENS) (Walsh and Zemper, 2019). The ENS is an extensive and complex neuronal network along the wall of the GI tract, composed of neurons and glia (Fleming et al., 2020; Sharkey and Mawe, 2023). It is well-known that both the digestive and immune defensive processes of the gastrointestinal (GI) tract are under ENS control (Sharkey and Mawe, 2023). However, how nerve cells impact the regulation of epithelial barrier function is not completely understood yet.

Previous studies have demonstrated that enteric neurons through

* Corresponding author. Hanzeplein 1, EA11, 9713 GZ, Groningen, the Netherlands.
E-mail address: x.chen@umcg.nl (X. Chen).

https://doi.org/10.1016/j.crfs.2024.100851
Received 16 July 2024; Received in revised form 29 August 2024; Accepted 12 September 2024
Available online 13 September 2024

peptide secretion indirectly influence intestinal paracellular permeability and intestinal cell proliferation to regulate gut barrier function (Neunlist et al., 2008). The release of vasoactive intestinal peptide (VIP) by enteric neurons reduced paracellular permeability and enhanced TJ gene *ZO-1* expression in Caco2 and HT29-Cl.16E monolayers (Neunlist et al., 2003). Also, neuropeptide Y (NPY) produced by submucosal neurons has been shown to regulate intestinal epithelial permeability via G protein-coupled receptors Y1 and Y2. This NPY also has an indirect effect on epithelium by modulating cytokine production (Chandrasekharan et al., 2013). Some clinical studies also suggest an important role for nerve cells in the barrier function of the gut epithelium. Both nerve regulation and immune responses have been shown to play key roles in the repair of the intestinal barrier after a flare in inflammatory bowel disease (IBD) patients (You et al., 2021). Based on these studies, it is generally assumed that nerve cells do influence intestinal epithelial barrier function, but how and whether they directly protect against damage by barrier-disrupting agents is still unknown.

To gain more insight into the interaction and protective effects of nerve cells for damage done by epithelial barrier disrupting agents we developed a co-culture system comprising of T84 intestinal epithelial cells and SH-SY5Y neuroblastoma cells. SH-SY5Y cells have been widely used as neuronal cell models (Dravid et al., 2021). We built this co-culture system based on previous evidence suggesting that nerve cells can be promoted to differentiate into enteric neurons when co-cultured with intestinal epithelial cells (Satsu et al., 2001) to mimic the native ENS environment. Intestinal epithelial cells have been shown to produce neurotrophic factors such as brain-derived neurotrophic factor (BDNF) and nerve growth factor (NGF) (Liu, 2018; Singh, 2023), especially BDNF, can efficiently promote the differentiation of SH-SY5Y cells (Bilginer Kartal and Arslan Yildiz, 2024). The possible protective effects of nerve cells on transepithelial electrical resistance (TEER) and the expression of TJ proteins and TJs-related genes in gut epithelial cells were tested after exposure of the cells to the barrier-disrupting agent calcium ionophores A23187. Additionally, the expression of proteins and genes involved in the regulation of the gut barrier function in nerve cells was also determined. Furthermore, we compared the rescuing effects of nerve cells with those of the human milk oligosaccharides (hMOs) 2′-fucosyllactose (2′-FL) and 3-fucosyllactose (3-FL) which are known to protect against barrier disruption (Kim et al., 2023). Also, we determined how the hMOs influence the regulation of proteins and genes associated with gut barrier function in the presence of nerve cells. The effect of hMOs on the interplay between the intestinal epithelium and nerve cells is largely unexplored and our study therewith contributes to a better knowledge of how hMOs and nerve cells contribute to the maintenance of an adequate gut barrier function.

2. Materials and methods

2.1. Human milk oligosaccharides

The human milk oligosaccharides (hMOs) 2′-fucosyllactose (2′-FL) and 3-fucosyllactose (3-FL) were provided by FrieslandCampina (Wageningen, the Netherlands). An overview of the hMO structures is shown in Table 1 (Kong et al., 2020). 2′-FL and 3-FL were dissolved in the T84 cell culture medium at a concentration of 2 mg/mL before performing the experiments. The applied dose was based on our group's previous study, which found that 2 mg/mL 2′-FL had a protective effect on the T84 intestinal barrier (Figueroa-Lozano et al., 2021). In this study, the same dose was also used for 3-FL to compare the impact of these two individual hMOs on gut barrier function.

2.2. Cell culture

The human colorectal carcinoma epithelial cell line T84 between passages 11–23 and the human neuroblastoma cell line SH-SY5Y between passages 52–67 were used in all experiments. Cells were confirmed to be mycoplasma free. T84 cells were cultured in Dulbecco's Modified Eagle Medium: Nutrient Mixture F-12 with 15 mM HEPES (DMEM/F-12, HEPES) (Gibco, Grand Island, NY USA) supplemented with 10% heat-deactivated fetal bovine serum (Serana Europe GmbH, Pessin, Germany) and 60 μg/mL gentamicin solution (Capricorn Scientific GmbH, Ebsdorfergrund, Germany). SH-SY5Y cells were cultured in DMEM/F-12, HEPES supplemented with 10% heat-deactivated fetal bovine serum, 1% Penicillin Streptomycin (Gibco, Grand Island, NY USA), and 1% 200 mM L-Glutamine (Lonza, Verviers, Belgium). These two cell lines were maintained at 37 °C with 5% CO_2. Medium was changed every other day. When the T84 cells and SH-SY5Y cells were grown to 80% confluency, cells were passaged. This required treatment with 0.1% and 0.05% trypsin-EDTA (Gibco, Grand Island, NY USA).

Table 1
Overview of the structures of hMOs applied in this study.

HMOs	Structure*
2'-fucosyllactose (2'-FL)	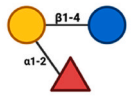
3-fucosyllactose (3-FL)	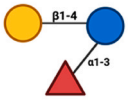

*Building blocks: 

For co-cultures of nerve cells and gut epithelial cells, T84 and SH-SY5Y cells were seeded in 12-well plates at ratios of 29:1 and 14:1, with a total of 100,000 cells per well and a final volume of 1.5 mL. The co-cultures were kept for two weeks in the T84 cells' complete medium, and the medium was replaced every other day. The seeding ratios were selected to avoid overgrowth and to achieve stable growth. After a growth period of two weeks, T84 and SH-SY5Y cells seeded at ratios of 29:1 and 14:1 approximately grew to the ratios of 4:1 and 3:1, respectively. To disrupt the barrier of the cells, we added 4 μM of A23187 for 24 h. T84 monolayers treated with medium only and treated with A23187 served as untreated and positive control respectively. To study the effects of 2′-FL and 3-FL, each well was pre-incubated for 24 h with 1 mL of 2 mg/mL 2′-FL or 3-FL, followed by exposure to 4 μM A23187 stimulation for 24 h. At least five independent experiments were performed. After the treatment of cells with the hMOs and A23187 in 12-well plates, the cells were washed with cold Dulbecco's phosphate buffer saline (DPBS) (Gibco, Gaithersburg, MD USA) three times. Then the cells were lysed with 500 μL TRIzol reagent (Invitrogen, Carlsbad, CA USA) per well. The lysed samples were stored at −80 °C for PCR.

2.3. Transepithelial electrical resistance (TEER) measurement

A real-time electric cell-substrate impedance sensing system (ECIS, Applied BioPhysics TM model Zθ) at multiple frequencies of 400 Hz was applied to quantify TEER. T84 cells and SH-SY5Y cells were seeded with ratios of 29:1 and 14:1 in 96-well PET plates with gold electrodes (96W20idf PET, Applied Biophysics) at a density of a total of 10,000 cells per well in a final volume of 300 μL. The seeding ratios were chosen to obtain stable TEER, and the TEER reached the same level as the group with only T84 epithelial cells (Supplementary materials, Fig. 1a). Before seeding the cells, the plates were coated with 300 μL per well of a 2 mg/mL L-cysteine (Merck, Darmstadt, Germany) solution in DPBS (Gibco, Gaithersburg, MD USA) for half an hour at room temperature (RT).

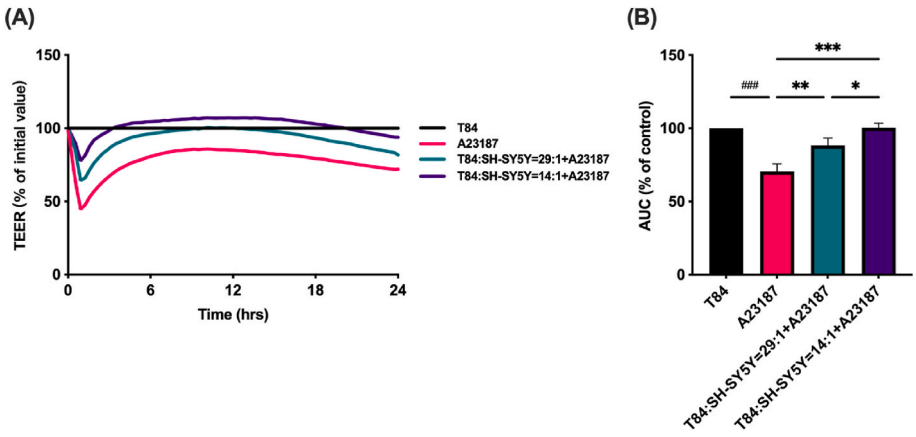

Fig. 1. The protective effect of SH-SY5Y nerve cells on calcium ionophore A23187-induced disruption of gut epithelial barrier function. The gut epithelial T84 and SH-SY5Y nerve cells were seeded at ratios of 29:1 and 14:1. Two weeks later, 4 μM A23187 was added for 24 h to the confluent monolayers of co-cultured T84 and SH-SY5Y cells. The T84 cell monolayer without any treatment was used as an untreated control, and T84 cells treated with A23187 were used as a positive control. (A). The relative TEER value changes after the addition of A23187 compared with the untreated control measured by ECIS. (B). The calculated area under the curve (AUC) of the untreated control was set at 100%. The AUC of the A23187-induced disruption in the co-cultures was compared with that of the T84 cultures or that of the untreated controls. Statistical differences between the untreated control and the positive control, as well as between the positive control and the different conditions, were determined. Data from six independent experiments are presented as mean ± SEM. $^{###}$ ($p < 0.001$) vs. untreated control; * ($p < 0.05$), ** ($p < 0.01$), or *** ($p < 0.001$) vs. positive control.

Subsequently, the plates underwent two washing steps in Dulbecco's modified Eagle's medium (DMEM) containing 4.5 g/L glucose, 4 mM L-glutamine, and 1 mM sodium pyruvate (Gibco, Grand Island, NY, USA). Next, the plates were coated with 300 μL DMEM with 1% type I bovine collagen (PureCol®, Advanced BioMatrix, San Diego, CA USA) and 0.1% bovine serum albumin (BSA) (Sigma-Aldrich, St. Louis, MO USA). The plates were left overnight at room temperature.

To establish a stable TEER of the intestinal monolayer, the co-cultured T84 and SH-SY5Y cells were kept at 37 °C with 5% CO_2 for two weeks. T84 cells' complete medium was used in the co-culture monolayers, and the medium was changed every other day. To stabilize the cell resistance, the plates were placed in the ECIS device for an entire night prior to the start of the experiments. The TEER was continuously monitored during the whole experimental period. To disrupt the gut barrier, cells were challenged with the gut barrier disruptor calcium ionophores A23187 (Sigma-Aldrich, St.Louis, MO USA). To this end, the co-cultured T84 and SH-SY5Y cell monolayers were treated with 4 μM A23187 for 24 h. At least five independent experiments were performed with three technical replicates per group. The area under the curve (AUC) was calculated to identify the changes in TEER following treatment with A23187 under various experimental conditions.

2.4. RNA isolation and reverse transcription

For RNA isolation, firstly, thawed lysed samples and the total RNA was isolated according to the TRIzol Reagent User Guide (Pub.No. MAN0001271 C.0). Total extracted RNA was dissolved in nuclease-free diethylpyrocarbonate (DEPC)-treated water (Life Technologies, Austin, USA). A NanoPhotometer® N60 (Implen GmbH, Munich, Germany) was applied to detect the concentration and purity of RNA. An aliquot of 500 ng RNA was utilized to synthesize reverse transcriptase cDNA. All reagents applied in the reverse transcription process were purchased from Thermo Fisher Scientific Inc., Vilnius, Lithuania. The reverse transcription was carried out according to the following procedures. The extracted RNA was first treated with DNAse following the manufacturer's instructions to remove the genomic DNA from RNA preparations. Then 200 ng of Random Hexamer Primers were added to DNAse-treated RNA, and the mixture was incubated at 65 °C for 5 min followed by cooling on ice for 2–3 min. Later, 4 μL 5X Reaction Buffer, 0.5 μL (20 U) RiboLock RNase Inhibitor, 2 μL dNTP mix (10 mM each), and 1 μL (200 U) RevertAid Reverse Transcriptase were added to each sample obtaining a final volume of 20 μL. Finally, the mixtures were incubated at 25 °C for 10 min, 42 °C for 60 min, and 70 °C for 10 min. All heating procedures were performed in a Biometra TAdvanced Thermocycler (Biometra GmbH, Göttingen, Germany). The cDNA samples were stored at −20 °C until use.

2.5. Quantitative polymerase chain reaction (qPCR)

The primer sequences of *CLDN1*, *CLDN2*, *CLDN3*, *CLDN4*, *OCLN*, *ZO-1*, *VIP*, and *NPY* are listed in Table 2. The procedure was as follows. A sample of 5 μL of 20x diluted cDNA with 5 μL of FastStart Universal SYBR® Green Master (Roche Diagnostics GmbH, Mannheim, Germany) with 6 μM primer was mixed. Genes expression was performed in 384-well PCR plates with a ViiA7 Real-Time PCR system (Applied Biosystems, Foster City, CA USA) following a 40-cycle protocol consisting of 15 s of denaturation at 95 °C, 30 s of primer annealing at 60 °C, and 30 s of extension at 72 °C, along with a melting curve. The housekeeping gene *GAPDH* was used to standardize the gene expression levels. The fold changes in gene expression of every group were calculated by the $2^{-\Delta\Delta CT}$ method.

2.6. Immunofluorescence staining and confocal microscopy

For immunofluorescence staining, cells were seeded in round microscopical coverslips and were put into 12-well plates. T84 and SH-SY5Y cells were seeded at ratios of 29:1 and 14:1, with a total of 100,000 cells per well and a final volume of 1.5 mL. Cells were maintained until reaching 70–80% confluency. Then the cells were incubated with medium or hMOs followed by A23187 exposure. Subsequently, the cells were washed twice with cold DPBS and fixed with 4% (w/v) paraformaldehyde (PFA) (Sigma-Aldrich, St. Louis, MO, USA) for 15–20 min at room temperature (RT). This was followed by 5 min of permeabilization with 0.1% (v/v) Triton X-100. Then, the cells were incubated at RT for 1 h with a blocking buffer composed of 1% (w/v) BSA (Sigma-Aldrich, St. Louis, MO, USA) and 0.1% (v/v) Tween 20 (Sigma-Aldrich, St. Louis, MO, USA) in PBS. After overnight incubation with the primary antibody for claudin-1 (Claudin1 Monoclonal Antibody, 1:200, Thermo Fisher Scientific) and VIP (VIP Polyclonal Antibody, 1:200, Thermo Fisher Scientific) at 4 °C, the cells were washed 3 times with DPBS, and incubated with secondary antibody Fluorescein

Table 2
Primer sequences used for real-time qPCR.

Primer	Forward (5'→3')	Reverse (5'→3')
Glyceraldehyde-3-phosphate dehydrogenase (GAPDH)	AGCCACATCGCTCAGACAC	GCCCAATACGACCAAATCC
Claudin-1 (CLDN1)	GATGAGGTGCAGAAGATGAG	GGACAGGAACAGCAAAGTAG
Claudin-2 (CLDN2)	CAGTGCAATCTCCTCCCTGG	GTCTTTGGCTCGGGATTCCT
Claudin-3 (CLDN3)	CTGCTCTGCTGCTCGTGTC	CGTAGTCCTTGCGGTCGTAG
Claudin-4 (CLDN4)	GCTGCTTTGCTGCAACTGTC	CTTGGCGGAGTAAGGCTTGT
Occludin (OCLN)	CTATAAATCCACGCCGGTTC	TATTCCTGTAGGCCAGTGTC
Zonula occludens-I (ZO-1)	TGCCTCTGAGAGAGACGACA	TCTCTACTCCGGAGACTGCC
Vasoactive Intestinal Peptide (VIP)	AATGGAAAGAGGAGCAGTGAGG	AACTCTTCTGGAAAGTCGGGAG
Neuropeptide Y (NPY)	GCTGCGACACTACATCAACCT	AAATCAGTGTCTCTGGGCTGG

goat anti-mouse IgG (H + L) (1:400, Thermo Fisher Scientific) and Texas Red goat anti-rabbit IgG (H + L) (1:300, Thermo Fisher Scientific) in the dark for 1 h at RT. The cells were then washed 3 times with DPBS, and the cell nuclei were stained with DAPI (1:5000, Sigma) followed by 3 washes with DPBS.

A Leica SP8 confocal laser microscope (Leica Microsystems, Wetzlar, Germany) with HC PL APO CS2 63 × /1.4 oil objective was applied to capture the immunofluorescence images. DAPI was excited at 405 nm and emitted at 410–450 nm (blue); FITC was excited at 495 nm and emitted at 517 nm (green); Texas Red was excited at 594 nm and emitted at 613 nm (red). The average immunofluorescence of claudin-1 and VIP was quantified by ImageJ.JS (Version 0.5.7). The Integrated density of each protein was measured and plotted as the fold-change of Integrated density among different conditions compared to the control.

2.7. Statistical analyses

Statistical analyses were performed using GraphPad Prism version 10.1.1. Normal distribution of the data was assessed using the Shapiro-Wilk test. The data were normally distributed. Therefore, data are expressed as the mean ± standard error of the mean (SEM) of at least five independent experiments. In all experiments, statistical significance was determined using one-way ANOVA with Holm-Šídák's multiple comparison test. A p-value <0.05 was considered significant. $^{\#}$ or * ($p < 0.05$), $^{\#\#}$ or ** ($p < 0.01$), $^{\#\#\#}$ or ***($p < 0.001$), $^{\#\#\#\#}$ or **** ($p < 0.0001$).

3. Results

3.1. The presence of higher numbers of nerve cells prevents nerve-intestinal barrier disruption induced by calcium ionophore A23187

To test the potential protective effect of nerve cells on intestinal barrier function, epithelial T84 cells were co-cultured with gradually increasing numbers of neuroblastoma SH-SY5Y cells for two weeks. Afterward, the confluent monolayers were stimulated with the gut barrier disruptor A23187 for 24 h, during which time TEER was measured.

Before the A23187 treatment, the TEER of T84 cells and T84/SH-SY5Y co-cultures reached almost the same level (Supplementary materials, Fig. 1a). Fig. 1A shows the relative TEER change following the addition of A23187 measured by ECIS in comparison to the untreated control. Based on the TEER changes, the area under the curve (AUC) was calculated. As shown in Fig. 1B, 4 μM A23187 significantly reduced AUC in T84 cell monolayers by 29.42% ($p < 0.001$) compared to the untreated control. The disrupting effects of A23187 were attenuated by the presence of nerve cells in a nerve cell concentration-dependent manner (Fig. 1B). The A23187-induced disruption in co-cultures at a ratio of 29:1 was only 19.10% and statistically significantly less disrupted compared to that of gut epithelial T84 cells only ($p < 0.01$). With the higher concentration of SH-SY5Y cells in a 14:1 ratio the A23187-induced disruption in the co-culture was only 5.82%. This disruption was statistically significantly less compared to that of gut epithelial T84 cells only ($p < 0.001$) and the T84:SHSY5Y = 29:1 monolayer ($p < 0.05$).

3.2. Higher numbers of nerve cells co-cultured with gut epithelial cells can prevent the A23187-induced overexpression of CLDN1, CLDN4, VIP and NPY

In addition to the TEER measurements, we also quantified the expression of intestinal barrier-regulating genes in T84 and SH-SY5Y cells (Fig. 2).

A23187 significantly upregulated TJs-genes. *CLDN1* expression was enhanced by A23187 2.71-fold ($p < 0.0001$) in T84 epithelial cells. This increase in *CLDN1* gene expression was attenuated in the presence of SH-SY5Y nerve cells and dependent on the concentration of nerve cells. Compared to A23187-exposed T84 epithelial cells, the co-cultures at a ratio of 29:1 and 14:1 showed a 0.91-fold ($p < 0.0001$) and 1.19-fold ($p < 0.0001$) lower *CLDN1* expression, respectively (Fig. 2A).

CLDN2 was virtually absent in T84 cells after exposure to A23187. This was not changed by the presence of SH-SY5Y nerve cells (Fig. 2B).

A23187 did not affect *CLDN3* expression in T84 epithelial cells. The co-cultures of T84 epithelial cells with SH-SY5Y nerve cells did not change significantly at a ratio of 29:1 but it was 0.47 times ($p < 0.05$) higher in the 29:1 ratio compared to the 14:1 co-culture (Fig. 2C).

CLDN4 expression was 2.02-fold ($p < 0.0001$) increased in T84 cells by the addition of A23187 (Fig. 2D). This A23187-induced enhancement in *CLDN4* was lower in the co-cultures with nerve cells and dependent on the concentration of nerve cells. In co-cultures of T84 cells and SH-SY5Y cells at a ratio of 29:1 and 14:1, *CLDN4* was 0.40-fold ($p < 0.05$) and 0.60-fold ($p < 0.001$) lower expressed, respectively.

The expression of *OCLN* was 1.97-fold (p < *0.0001*) increased in T84 cells exposed to A23187. This enhancement could be partially prevented in co-cultures with SH-SY5Y nerve cells, but this did not reach statistical significance (Fig. 2E).

Also, *ZO-1* expression was 2.10-fold ($p < 0.001$) enhanced in T84 cells after exposure to A23187. This upregulation was not changed by co-culture of T84 cells with SH-SY5Y cells at a ratio of 14:1 but this was even 0.77-fold ($p < 0.05$) higher than the A23187 exposed cells at a ratio of 29:1 (Fig. 2F).

We not only studied TJ genes but also studied expression of two nerve cell derived genes known to be involved in the regulation of barrier function. These are *VIP* and *NPY* (Chandrasekharan et al., 2013). A23187 significantly increased the expression of *VIP* in 1.53-fold ($p < 0.01$) in T84:SH-SY5Y = 29:1 co-culture while it was not statistically higher in the 14:1 ratio (Fig. 2G). We observed the same trend of expression in the *NPY* gene expression. The *NPY* expression was enhanced 1.62-fold ($p < 0.001$) in T84:SH-SY5Y = 29:1 co-culture after A23187 challenge. But the addition of more nerve cells co-cultured with T84 cells significantly lowered the *NPY* expression (Fig. 2H).

3.3. Nerve cells co-cultured with gut epithelial cells alter the A23187-induced overexpression of Claudin-1 and VIP proteins

Next, we determined the expression of claudin-1 as well as of VIP protein in T84 and SH-SY5Y cells by immunofluorescence staining

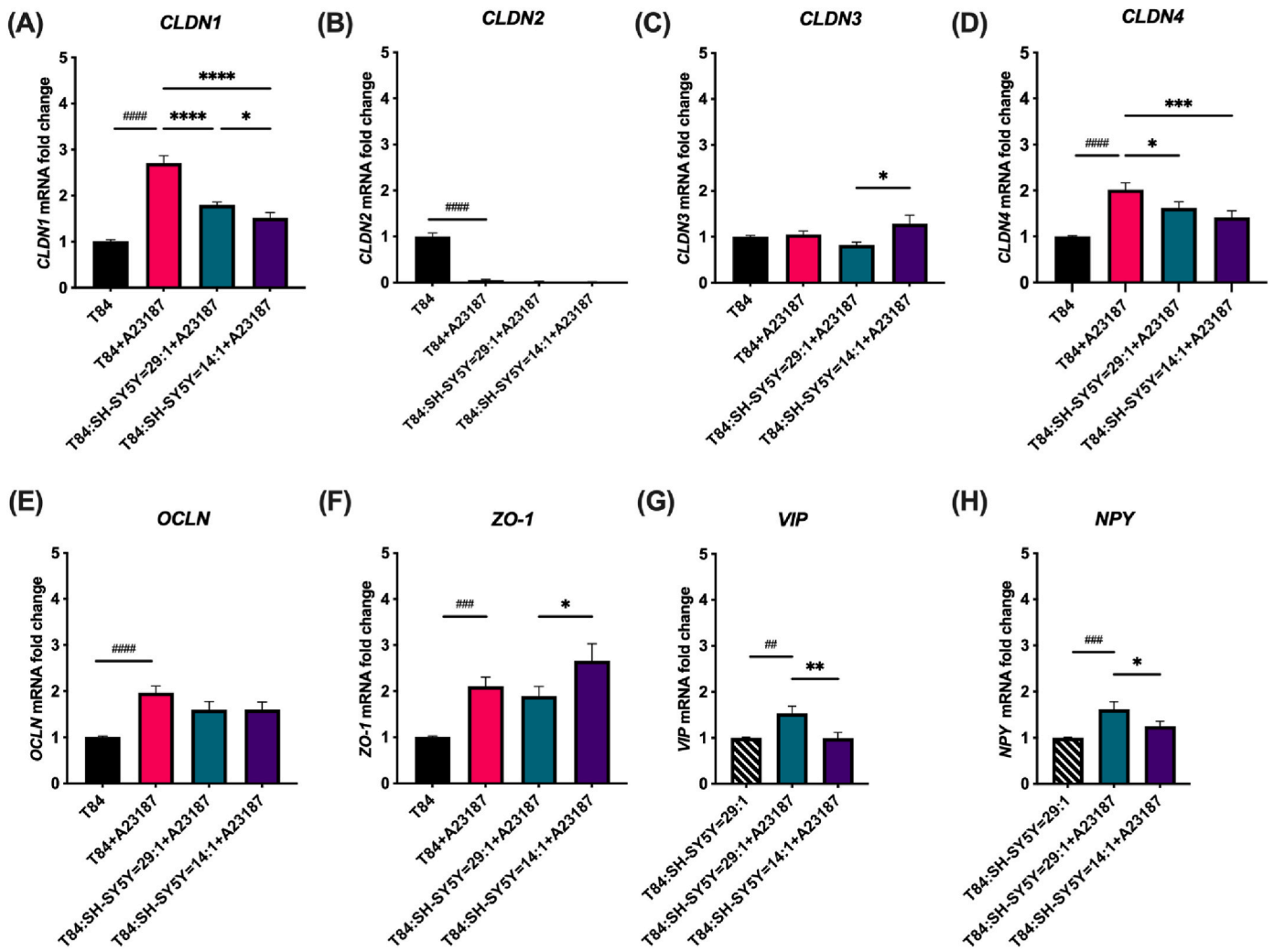

Fig. 2. The effect of SH-SY5Y cells on the expression of genes related to the regulation of the intestinal barrier in co-cultures of nerve cells and gut epithelial intestinal cells. The co-cultures were stimulated with 4 μM A23187 for 24 h. T84 cells without any treatment were used as the untreated control and T84 cells treated with A23187 were used as the positive control. The changes in expression of genes *CLDN1* (A), *CLDN2* (B), *CLDN3* (C), *CLDN4* (D), *OCLN* (E), *ZO-1* (F), *VIP* (G), and *NPY* (H) were quantified by qPCR. Statistical differences between the untreated control and the positive control; as well as between the positive control and the different conditions were determined. Data from at least five independent experiments are presented as mean ± SEM. $^{*}p < 0.05$, $^{\#\#}$ or $^{**}p < 0.01$, $^{\#\#\#}$ or $^{***}p < 0.001$, $^{\#\#\#\#}$ or $^{****}p < 0.0001$.

(Fig. 3). Fig. 3A shows that VIP is exclusively expressed in SH-SY5Y cells, and that claudin-1 is only expressed in T84 cells (Fig. 3B). T84 cells stimulated by A23187 upregulated the expression of the TJ protein claudin-1 (Fig. 3C). Its immunofluorescence intensity increased by 0.17-fold ($p < 0.05$, Fig. 3G). When SH-SY5Y cells were co-cultured with T84 cells at a low ratio of 29:1, it induced the production of both claudin-1 and VIP (Fig. 3D). Compared with A23187-exposed T84 cells only, claudin-1 expression was enhanced in A23187-exposed co-cultures of nerve cells and T84 cells (Fig. 3E and F), leading to a 0.31-fold and a 0.33-fold increase in its immunofluorescence intensity in cocultures of 29:1 and 14:1 respectively ($p < 0.05$, Fig. 3G). The intensity of VIP protein was enhanced to 1.43-fold by A23187 in T84:SH-SY5Y = 29:1 co-culture ($p < 0.01$), and this did not change in the T84:SH-SY5Y = 14:1 co-culture (Fig. 3E, F and 3H).

3.4. 2′-FL and 3-FL exert protective effects on A23187-induced disruption of gut epithelial cells

As it has been previously shown that some hMOs can protect gut epithelial cells from barrier disruption (Figueroa-Lozano et al., 2021), we exposed the gut epithelial cells and the co-cultures of gut epithelial cells with nerve cells to 2′-FL and 3-FL before exposure to 4 μM A23187. This was done to determine whether these hMOs might protect from barrier disruption and for comparison of the efficacy of protection with that of nerve cells. To this end, intestinal epithelial T84 cells and co-cultures of T84 and SH-SY5Y nerve cells were pre-incubated for 24 h with 2 mg/mL 2′-FL or 3-FL. Next, 4 μM A23187 was added for another 24 h.

Fig. 4A shows the dynamics of the alterations of TEER in T84 cells after the incubation with 2′-FL or 3-FL in the presence of A23187. The AUC of each line was calculated and shown in Fig. 4B. The addition of A23187 significantly disrupted the TEER and the AUC was decreased to 66.26% ($p < 0.0001$) compared with the untreated control. This disruption was prevented by pre-incubation with 2′-FL or 3-FL prior to the stimulation with A23187. In comparison to the positive control, 2′-FL and 3-FL rescued the TEER, as the AUC increased by 16.74% ($p < 0.05$) and 27.52% ($p < 0.001$), respectively.

This preventive effect of 2′-FL and 3-FL on A23187-induced barrier disruption was not observed in the co-cultures of T84 cells with SH-SY5Y cells irrespective of the ratio applied. Just like in the first series of experiments in Section 3.1 the presence of nerve cells as such resulted in a lower A23187-induced barrier disruption (Fig. 4C–F).

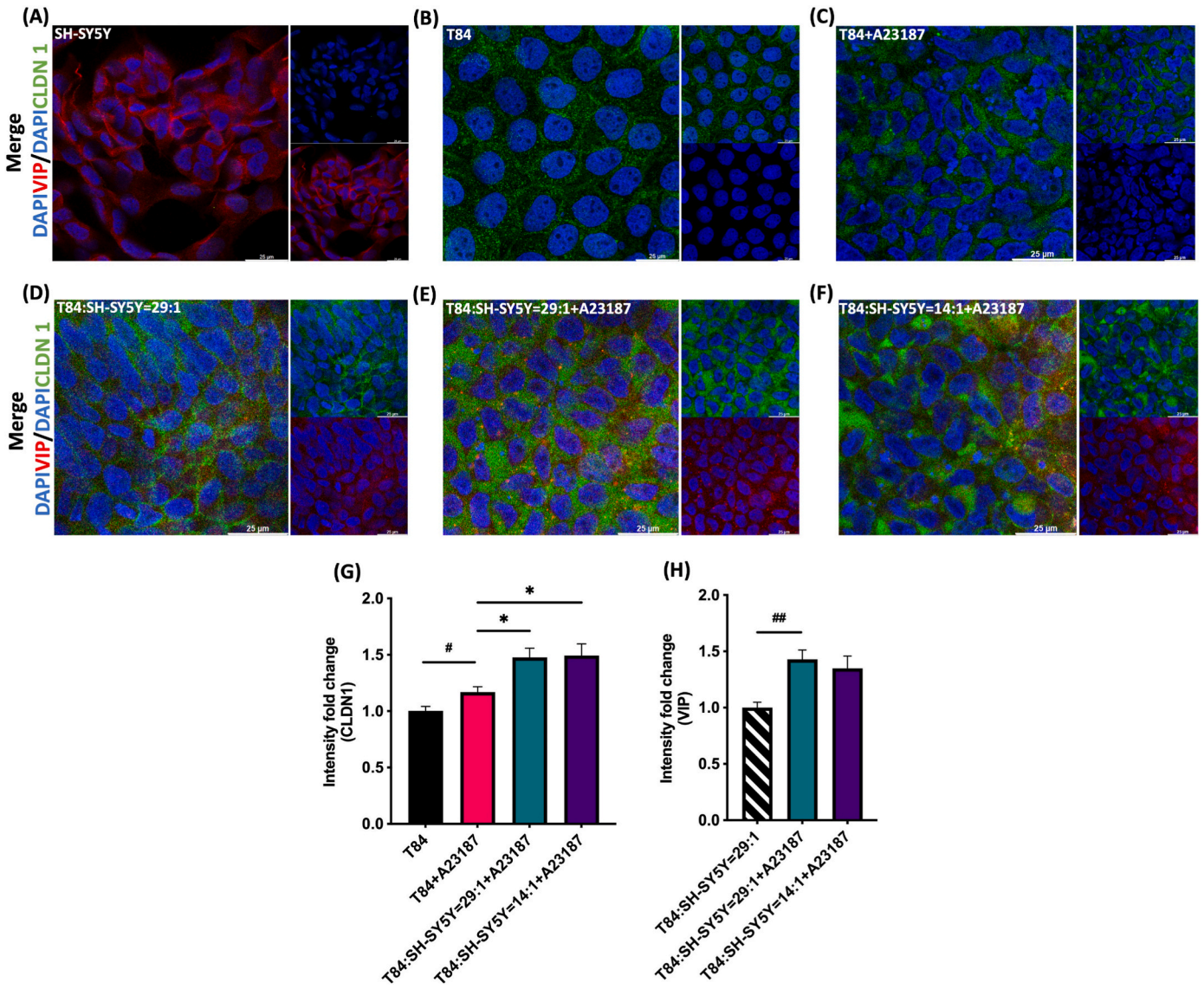

Fig. 3. The effect of nerve cells on the expression of claudin-1 and VIP protein in A23187-exposed co-cultures of gut epithelial T84 cells and nerve SH-SY5Y cells. T84 cells and co-cultures (T84:SH-SY5Y = 29:1 and 14:1) were incubated for two weeks followed by exposure to 4 μM A23187 for 24 h. For SH-SY5Y cells we used a five-day culture period to stain VIP to avoid too strong growth and inability to stain the multiple layers of cells. To compare claudin-1 expression in T84 and co-cultures, A23187-induced T84 cells served as positive control. To compare VIP expression in co-cultures containing different numbers of nerve cells, A23187-induced T84:SH-SY5Y = 29:1 co-cultures were applied as positive control. Immunofluorescence staining was applied to stain claudin-1 (claudin-1, green; cell nuclei, blue) and VIP (VIP, red; cell nuclei, blue). The immunofluorescence intensity of claudin-1 and VIP were quantified by Image J. Statistical differences between the untreated control and the positive control; as well as between the positive control and the different conditions were determined. Data from at least five different areas of the figures are presented as mean ± SEM. $^{\#}$ or $^{*}p < 0.05$, $^{\#\#}p < 0.01$. (For interpretation of the references to color in this figure legend, the reader is referred to the Web version of this article.)

3.5. 2′-FL attenuated A23187-induced overexpression of CLDN4 and OCLN, whereas 3-FL promoted A23187-induced overexpression of ZO-1 in gut epithelial T84 cells

Next, we studied TJs regulation of 2′-FL and 3-FL on the A23187-disrupted intestinal barrier. These analyses were done separately for T84 cells (Fig. 5) and for co-cultures of T84 and SH-SY5Ycells in a ratio of 29:1 (Section 3.6, Fig. 6), and for co-cultures of T84 and SH-SY5Y cells in a ratio of 14:1 (Section 3.7, Fig. 7).

The expression of *CLDN1* was significantly upregulated by 2.93-fold ($p < 0.0001$) in T84 cells stimulated with A23187 compared to untreated control, however, this upregulation could not be modulated by 2′-FL as well as 3-FL (Fig. 5A).

A23187 strongly suppressed the expression of *CLDN2* in T84 cells. The hMOs 2′-FL and 3-FL were unable to regulate *CLDN2* (Fig. 5B).

The expression of *CLDN3* was not affected by A23187 treatment; however, it was significantly increased to 1.26-fold ($p < 0.05$) after 3-FL pre-treatment of A23187-induced T84 cells compared to the positive control (Fig. 5C).

For *CLDN4* expression, A23187 significantly induced higher *CLDN4* expression by 2.04-fold in T84 epithelial cells ($p < 0.0001$), but this high level of expression was inhibited by 2′-FL to a 1.57-fold change ($p < 0.0001$) (Fig. 5D).

A 2.09-fold ($p < 0.0001$) increase in *OCLN* expression was found in A23187-exposed T84 epithelial cells. This high expression was significantly prevented to 1.83-fold as well as 1.84-fold ($p < 0.001$) by 2′-FL and 3FL, respectively (Fig. 5E).

When A23187 was added to stimulate T84 cells, the *ZO-1* expression increased 2.27-fold ($p < 0.001$) compared with untreated control. The pre-exposure to 3-FL even enhanced the *ZO-1* expression to 2.601-fold

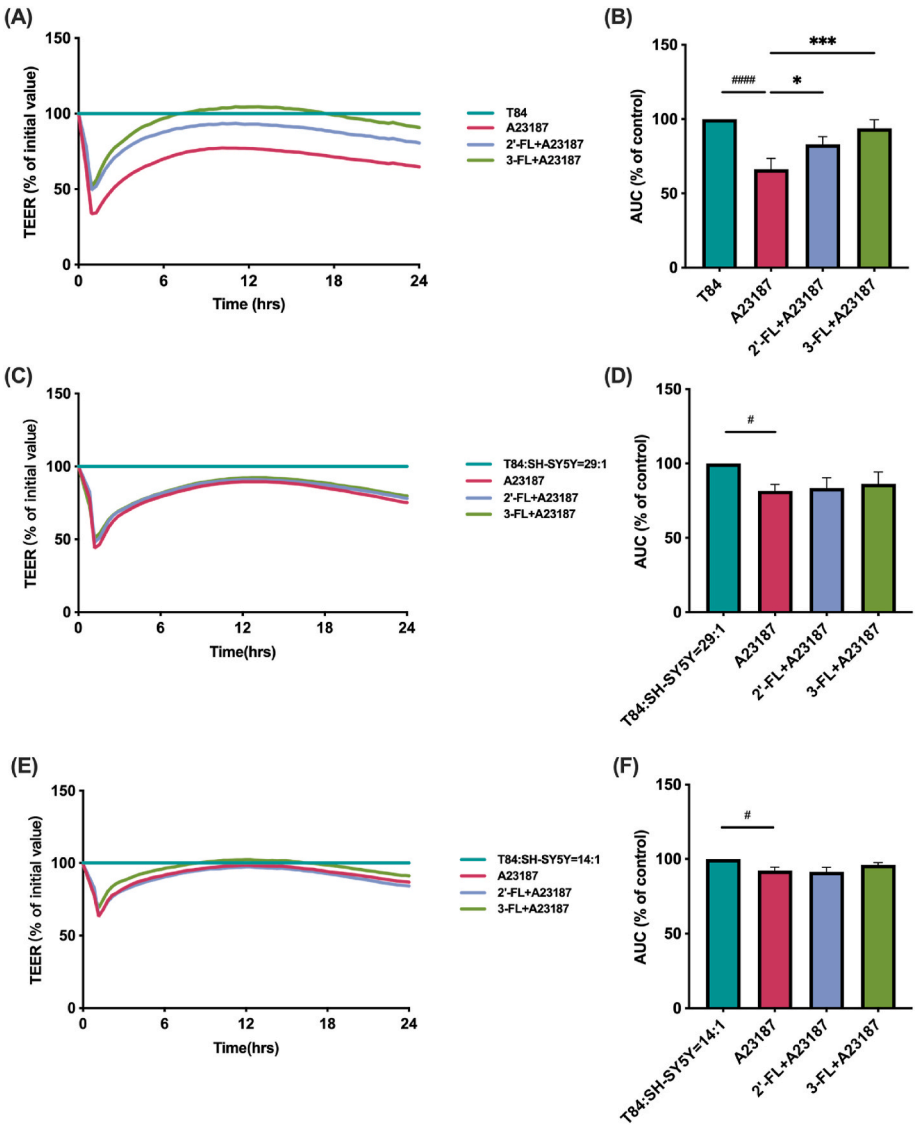

Fig. 4. The protective effect of 2′-FL and 3-FL on calcium ionophore A23187 gut epithelial barrier disruption in the presence and absence of nerve cells. The T84 gut epithelial cells and SH-SY5Y nerve cells were seeded at ratios of 29:1 and 14:1 for two weeks. Afterward, the confluent monolayers of co-cultured T84 and SH-SY5Y cells or T84 cells only were incubated with 2 mg/mL 2′-FL or 3-FL for 24 h followed by the addition of 4 μM A23187 for 24 h. The monolayers without any treatment were used as the untreated control and monolayers treated with A23187 were used as the positive control. (A), (C), and (E) show the changes in relative TEER values of T84 monolayers, T84:SH-SY5Y = 29:1 monolayer, and T84:SH-SY5Y = 14:1 monolayer, respectively, pre-cultured with hMOs after the addition of A23187 compared to untreated controls. (B), (D), and (F) show the calculated area under the curve (AUC) of (A), (C), and (E), respectively. The AUC of untreated control was set as 100%. The % AUC of hMOs pre-incubated and A23187 treated monolayers was compared with that of the untreated control. Statistical differences between the untreated control and the positive control; as well as between the positive control and the different conditions were determined. Data from six independent experiments are presented as mean ± SEM. $^{\#}$ or * ($p < 0.05$), *** ($p < 0.001$), $^{\#\#\#\#}$ ($p < 0.0001$).

($p < 0.05$) (Fig. 5F).

3.6. 3-FL enhanced A23187-induced overexpression of CLDN3 when T84 cells were co-cultured with SH-SY5Y cells at a seeding ratio of 29:1

Next, the gut epithelial cells T84 were co-cultured with nerve cells SH-SY5Y in a ratio of 29:1. The expression of intestinal barrier regulation-related genes in T84 and SH-SY5Y cells was determined to have more insight into the potential effects of 2′-FL and 3-FL on preventing TJ-regulation induced by A23187 in the presence of lower numbers of nerve cells. The epithelium of T84 cells co-cultured with SH-SY5Y cells at a ratio of 29:1 was first incubated by 2′-FL and 3-FL for 24 h followed by the addition of A23187.

A23187 significantly enhanced *CLDN1* expression 3.27-fold ($p <$ 0.0001). However, the expression of *CLDN1* was not regulated by any of the hMOs (Fig. 6A).

The expression of *CLDN2* was also almost completely inhibited by A23187. This inhibition was so strong that 2′-FL and 3-FL could not play any role in the regulation of *CLDN2* (Fig. 6B).

CLDN3 expression was increased 1.17-fold ($p < 0.05$) in the co-cultures with the addition of A23187. The pre-incubation of 3-FL enhanced *CLDN3* expression 1.33-fold ($p < 0.05$) (Fig. 6C) while 2′-FL had no effect.

A23187 promoted *CLDN4* expression 1.59-fold (Fig. 6D) and *OCLN* expression 2.18-fold (Fig. 6E) in the co-cultures of the nerve and epithelial cells (both $p < 0.0001$). The upregulation of these two TJ genes was not affected by 2′-FL and 3-FL.

Addition of A23187 to untreated co-cultures significantly increased *ZO-1* expression 2.77-fold ($p < 0.0001$). Pre-exposure to 3-FL of the co-cultures stimulated by A23187 tended to increase *ZO-1* expression ($p =$

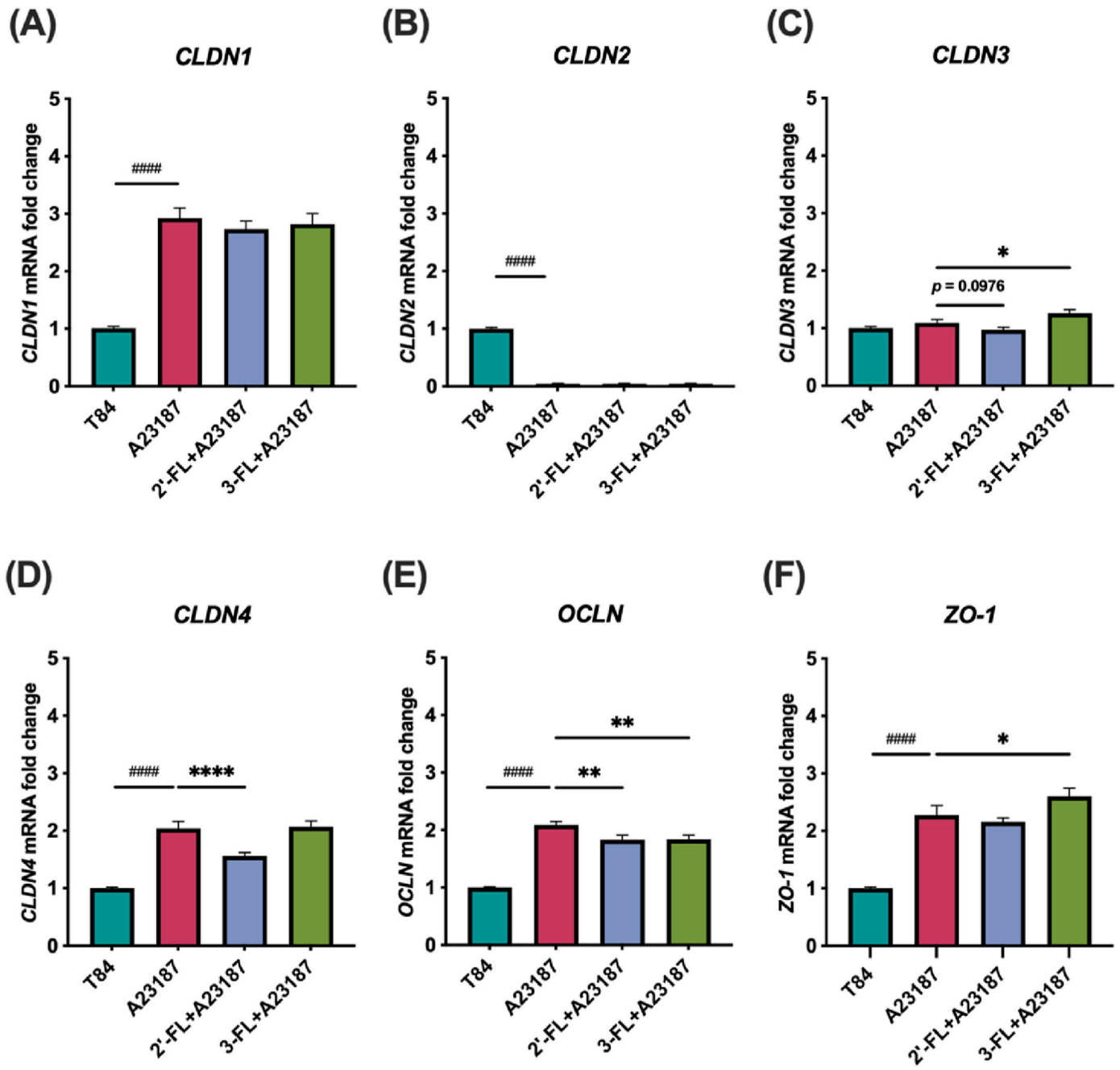

Fig. 5. The effect of 2′-FL and 3-FL on the expression of TJs genes in gut epithelial T84 cells. T84 cells were pre-treated with 2 mg/mL 2′-FL or 3-FL for 24 h, then 4 μM A23187 were added for 24 h of incubation. T84 cells without any treatment were used as the untreated control and T84 cells treated with A23187 were used as the positive control. The changes in expression of TJ genes *CLDN1* (A), *CLDN2* (B), *CLDN3* (C), *CLDN4* (D), *OCLN* (E) and *ZO-1* (F) were identified by qPCR. Statistical differences between the untreated control and the positive control; as well as between the positive control and the different conditions were determined. Data from at least five independent experiments are presented as mean ± SEM. * ($p < 0.05$), ** ($p < 0.01$), #### or **** ($p < 0.0001$).

0.0792) (Fig. 6F).

Fig. 6G and H demonstrate the expression of *VIP* and *NPY* associated with intestinal barrier modulation that are exclusively expressed in SH-SY5Y cells. In the 29:1 co-cultivation ratio of T84 and SH-SY5Y cells, A23187 significantly enhanced the expression of *VIP* and *NPY* by 1.53 and 1.57 times ($p < 0.05$), respectively. The hMOs 2′-FL and 3-FL did not change this regulation.

3.7. 2′-FL prevent the A23187-induced overexpression of CLDN1, CLDN3, CLDN4 and ZO-1 when T84 cells were co-cultured with SH-SY5Y cells at a seeding ratio of 14:1

Also, TJ expression and regulation in co-cultures of T84 epithelial cells and SH-SY5Y nerve cells at a 14:1 ratio were studied.

CLDN1 expression was 2.86-fold ($p < 0.0001$) upregulated by A23187. This upregulation of *CLDN1* induced by A23187 was prevented by 2′-FL to 2.36-fold ($p < 0.01$) (Fig. 7A).

A23187 almost completely blocked *CLDN2* expression (Fig. 7B). 2′-FL and 3-FL were unable to change this.

CLDN3 expression was significantly enhanced 1.51 times ($p <$

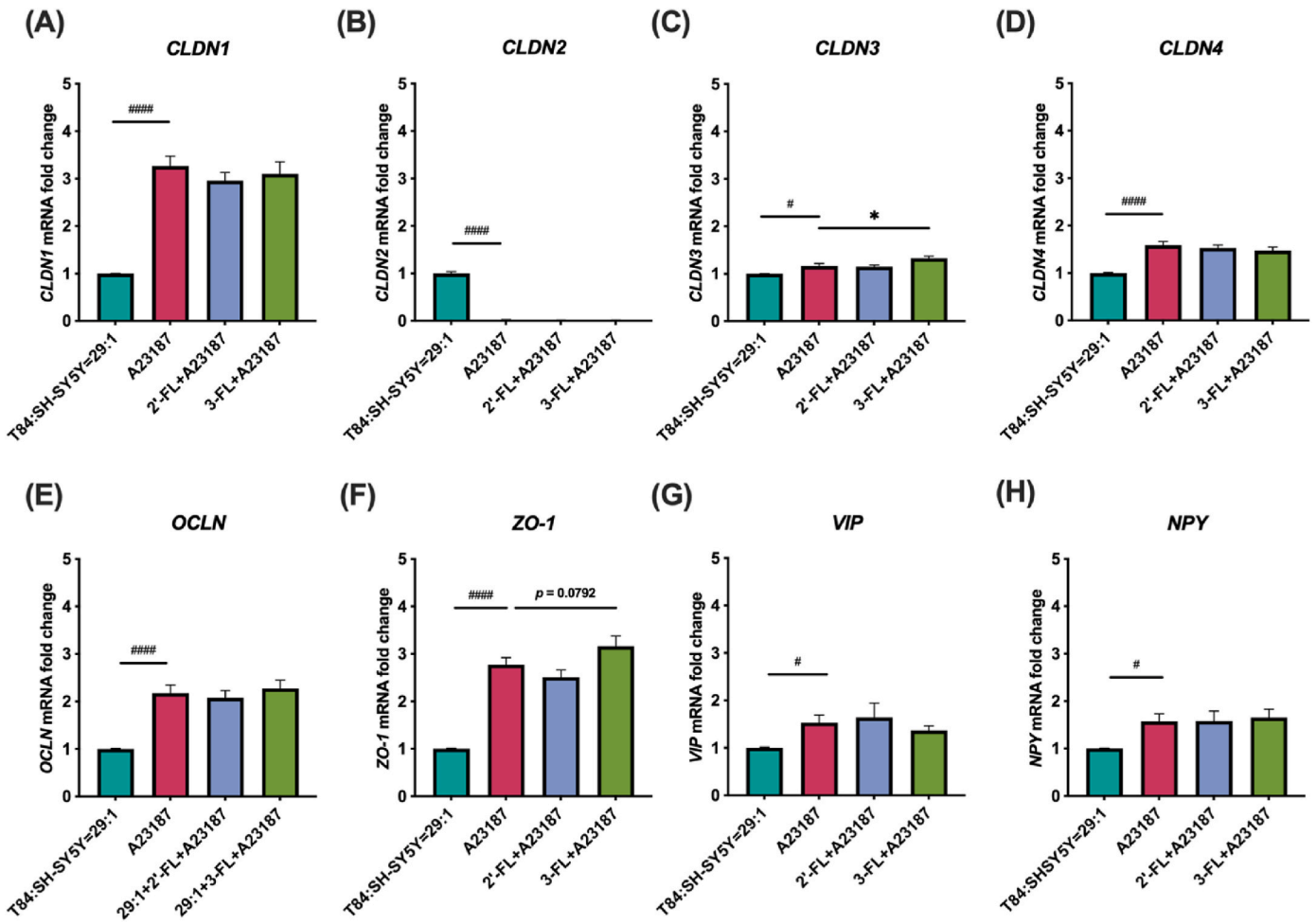

Fig. 6. The effect of 2′-FL and 3-FL on the expression of genes related to the regulation of the intestinal barrier in co-cultures of T84 gut epithelial cells and nerve cells in a ratio of 29:1. The co-culture monolayers were pre-treated with 2 mg/mL 2′-FL or 3-FL for 24 h followed by 4 μM A23187 stimulation for another 24 h. The monolayers without any treatment were used as untreated control and monolayers treated with A23187 were used as the positive control. The changes in expression of genes *CLDN1* (A), *CLDN2* (B), *CLDN3* (C), *CLDN4* (D), *OCLN* (E), *ZO-1* (F), *VIP* (G), and *NPY* (H) were identified by qPCR. Statistical differences between the untreated control and the positive control; as well as between the positive control and the different conditions were determined. Data from at least five independent experiments are presented as mean ± SEM. $^{\#}$ or * ($p < 0.05$), $^{\#\#\#\#}$ or **** ($p < 0.0001$).

0.0001) when exposed to A23187. 2′-FL and 3-FL attenuated this A23187 induced *CLDN3* overexpression which was 1.16-fold reduced by 2′-FL ($p < 0.0001$) and 1.28-fold lower with 3-FL ($p < 0.01$) (Fig. 7C).

CLDN4 was also highly expressed after the addition of A23187, which was 2.04-fold ($p < 0.0001$) higher than that of untreated controls. 2′-FL significantly reduced the expression of *CLDN4* to 1.58-fold ($p < 0.01$) while 3-FL had no effect (Fig. 7D).

Compared to the untreated control, *OCLN* expression in co-cultures of nerve cells and epithelium stimulated by A23187 led to a 2.73-fold higher expression ($p < 0.0001$). 2′-FL had a reducing effect on over-expression of *OCLN,* but this did not reach statistical significance ($p = 0.0874$), however, 3-FL had not such an effect (Fig. 7E).

Expression of *ZO-1* was elevated 3.38-fold ($p < 0.0001$) after the A23187 treatment compared to the untreated control. This high expression was decreased to 2.45-fold ($p < 0.05$) after the incubation with 2′-FL while 3-FL had not such an effect (Fig. 7F).

The expression of *VIP* and *NPY* are shown in Fig. 7G and H. When T84 cells were co-cultured with SH-SY5Y cells in a 14:1 ratio, A23187 did not affect *VIP* expression but tended to up-regulate *NPY* expression (*p= 0.0997*). 2′-FL and 3-FL pre-incubation did not show any regulations of *VIP* and *NPY* expression in A23187-stimulated co-cultures of nerve cells and gut epithelium.

3.8. 2′-FL and 3-FL differently modulate Claudin-1 and VIP protein expression in A23187-exposed co-cultures of T84 and SH-SY5Y cells

We also investigated the effects of 2′-FL and 3-FL on the protein levels of claudin-1 and VIP in A23187-treated T84 and SH-SY5Y cell co-cultures by immunofluorescence staining (Fig. 8). In T84 cells, 2′-FL attenuated the A23187-induced increase in claudin-1, while 3-FL promoted claudin-1 expression (Fig. 8A and B). In the co-cultures of T84:SHSY5Y = 29:1, 2′-FL significantly down-regulated A23187-induced claudin-1 and VIP overexpression ($p < 0.01$). 3-FL enhanced A23187-induced claudin-1 upregulation ($p < 0.01$) but did not significantly increase A23187-induced VIP overexpression (Fig. 8C and D). When more SH-SY5Y cells were seeded with T84 cells (T84:SHSY5Y = 14:1), the expression of claudin-1 was not influenced by A23187 and the pre-incubation of 2′-FL and 3-FL. But 3-FL promoted VIP expression, which fluorescence intensity significantly increased to a 2.14-fold change ($p < 0.001$, Fig. 8E and F).

4. Discussion

To the best of our knowledge, this is the first study in which crosstalk and the effects of nerve cells on intestinal barrier function are studied and demonstrated. We confirm the presence of paracrine crosstalk

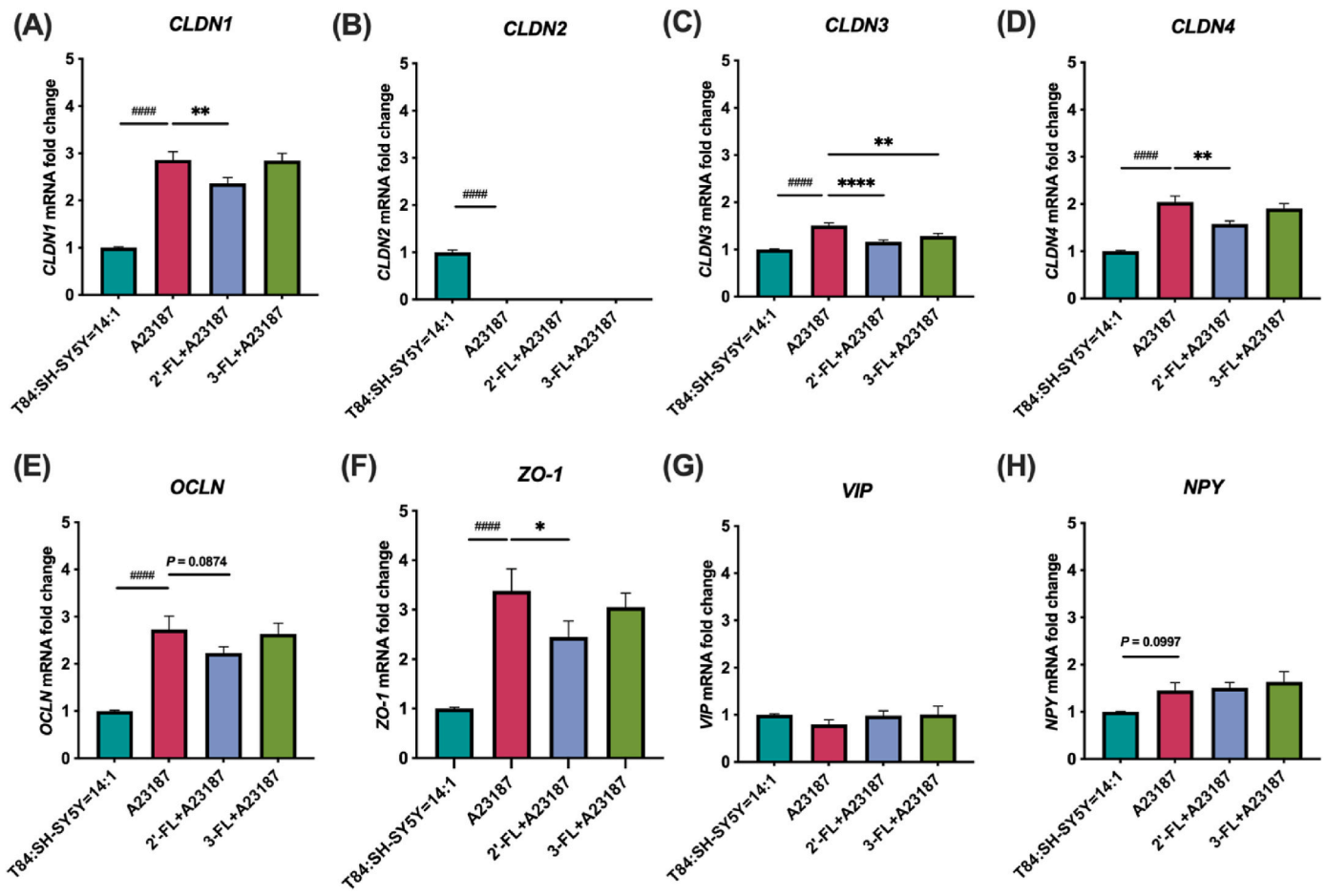

Fig. 7. The effect of 2′-FL and 3-FL on the expression of genes related to the regulation of the intestinal barrier in co-culture of T84 gut epithelial cells and nerve cells in a ratio of 14:1. The co-culture monolayers were pretreated with 2 mg/mL 2′-FL or 3-FL for 24 h followed by 4 μM A23187 stimulation for another 24 h. The monolayers without any treatment were used as the untreated control and monolayers treated with A23187 were used as the positive control. The changes in expression of genes *CLDN1* (A), *CLDN2* (B), *CLDN3* (C), *CLDN4* (D), *OCLN* (E), *ZO-1* (F), *VIP* (G), and *NPY* (H) were identified by qPCR. Statistical differences between the untreated control and the positive control; as well as between the positive control and the different conditions were determined. Data from at least five independent experiments are presented as mean ± SEM. * ($p < 0.05$), ** ($p < 0.01$), #### or **** ($p < 0.0001$).

between gut epithelial cells and nerve cells by the production of nerve cell-derived barrier-regulating molecules such as VIP and NPY. Also, we demonstrate the impact of direct contact between nerve cells and epithelium on rescuing barrier disruption by showing more protective effects when a higher number of nerve cells are present in the co-cultures with gut epithelial cells. The hMOs 2′-FL and 3-FL did not have an additional rescuing effect on A23187-induced barrier disruption in the presence of nerve cells, but the hMOs had a similar rescuing effect on ionophore-induced disruption in the absence of nerve cells. The impact on barrier function was highly dependent on TJ regulation (Chelakkot et al., 2018) which could partly be explained by the paracrine effects of the addition of nerve cells and partly by direct cellular interactions.

The formation of TJs between neighboring intestinal epithelial cells is essential for maintaining the integrity and function of the intestinal barrier. This barrier allows the penetration of nutrients and water but limits the entry of harmful substances (Chelakkot et al., 2018). The disruption of TJs results in the paracellular transport of undesired components from the lumen to the circulation which might negatively influence health. The TJ proteins play an important role in regulating the barrier function and maintaining health (Lee et al., 2018). The calcium ionophore A23187 applied in this study can increase intracellular calcium and activate the intracellular signal transduction protein kinase C (PKC) pathways. TJs are tightly modulated by the PKC pathway and this kinase disassembles the TJs eventually leading to gut barrier disruption (Fernández-Lainez et al., 2023; Lee et al., 2018). The reduction in TEER following A23187 exposure in cultures of T84 epithelial cells only proved the disruptor's damage to the gut epithelial barrier. However, the addition of nerve cells attenuated this disruption, with a higher concentration of SH-SY5Y cells demonstrating a stronger protective effect. Therefore, our data suggest that nerve cells may attenuate protein kinase C (PKC) pathways in the gut epithelial cells.

In a previous study it was found that the TEER of Caco-2 epithelial monolayers was significantly reduced, and the intestinal permeability was increased when Caco-2 cells were co-cultured with nerve PC12 cells (Satsu et al., 2001). However, no influence of neurotransmitters related to gut-barrier modulation secreted by PC12 cells was observed (Satsu et al., 2001). In our study, the addition of nerve cells as such did not influence the strength of the barrier in T84 cells. This is supported by the observation that before the start of the experiments, the TEER in cultures of T84 was similar to that of the co-cultures of T84 with the SH-SY5Y cells. This indicates that nerve cells may directly interact with gut epithelial cells to further modulate the gut barrier. Later, the same research group found that this reduction of TEER in Caco-2 cells was prevented by coculturing cycloheximide exposure of PC12 cells in the basolateral side of the trans-well (Satsu et al., 2003). Cycloheximide as an inhibitor of protein synthesis has been proven to alter protein degradation via the activation of protein kinase B (Dai et al., 2013). This suggests that certain protein changes in PC12 cells are involved in this TEER regulation (Satsu et al., 2003). Similarly, the addition of A23187 to our co-culture system may directly alter some unknown protein

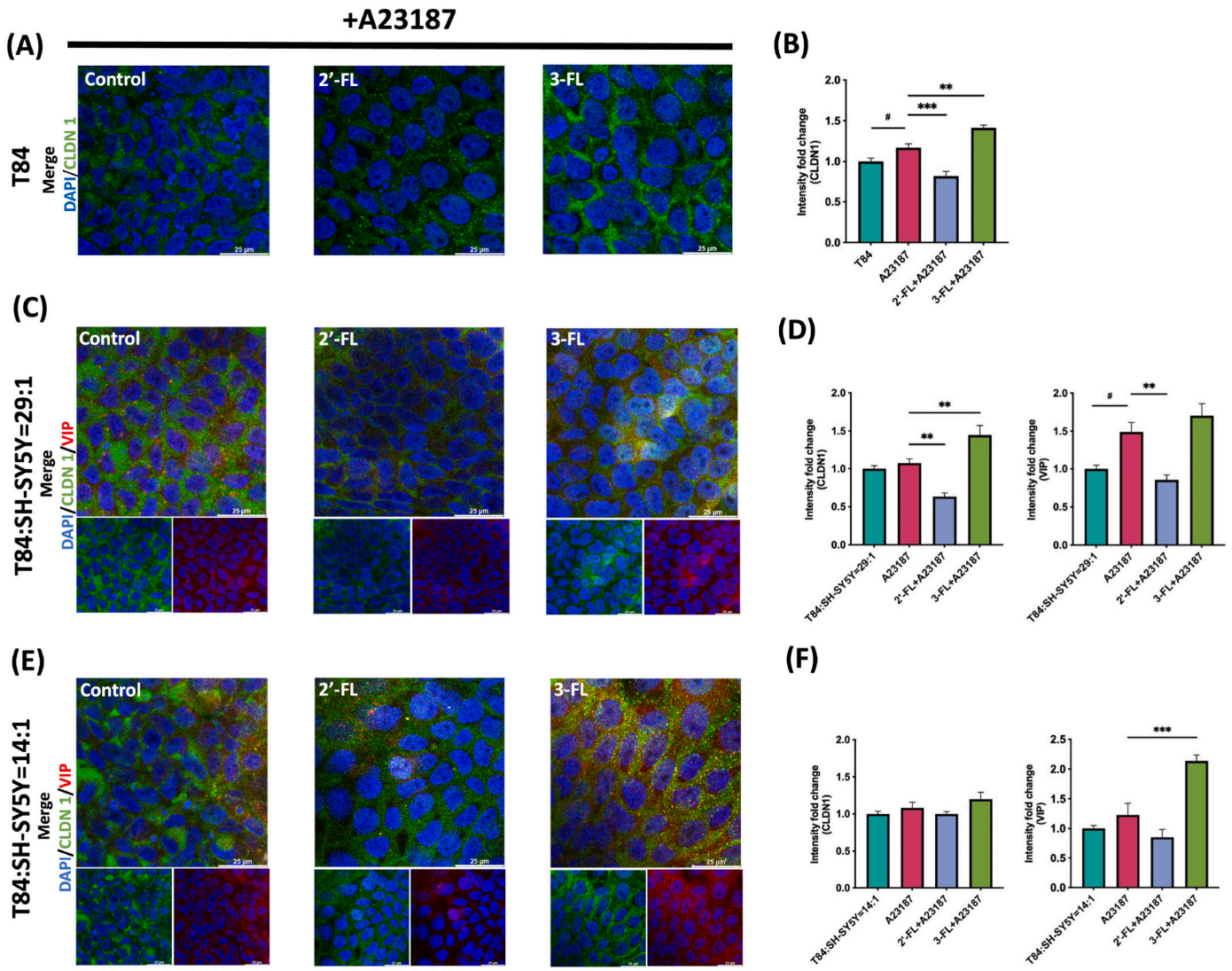

Fig. 8. The effect of 2′-FL and 3-FL on the expression of claudin-1 and VIP protein in A23187-disrupted T84 gut epithelial cells and co-cultures of nerve SH-SY5Y cells and T84 cells. T84 cells and co-cultures (T84:SH-SY5Y = 29:1 and 14:1) were kept for two weeks. Then the cells were incubated with 2 mg/mL 2′-FL and 3-FL for 24 h followed by 24 h-disruption by 4 μM A23187. To compare the possible different influences of 2′-FL and 3-FL on protein expression in T84 and co-cultures, A23187-induced T84 cells and A23187-exposed co-cultures served as positive control. Immunofluorescence staining was applied to label the claudin-1 (claudin-1, green; cell nuclei, blue) and VIP (VIP, red; cell nuclei, blue). The immunofluorescence intensity of claudin-1 and VIP were quantified by ImageJ. Statistical differences between the untreated control and the positive control; as well as between the positive control and the different conditions were determined. Data from at least five different areas of the figures are presented as mean ± SEM. $^{\#}p < 0.05$, $^{\#\#}$ or $^{**}p < 0.01$, $^{***}p < 0.001$. (For interpretation of the references to color in this figure legend, the reader is referred to the Web version of this article.)

synthesis in SH-SY5Y cells, and this alteration may prevent the disruption of TJs from A23187-induced kinase production and further protect TEER. The rescuing effects may also be attributed to the specific regulatory effects of nerve cells on the PKC pathway in T84 cells and the upregulation of TJ protein making T84 cells more resistant to disruption. This suggestion is supported by our immunofluorescence staining, where we found an increase in claudin-1 protein expression in the T84-SH-SY5Y co-cultures.

A23187 significantly upregulated *CLDN1*, *CLDN4*, and other TJ genes (*OCLN* and *ZO-1*) as well as claudin-1 protein in T84 cells, indicating that the gut epithelial cells may tend to express more TJs to compensate for the loss of TJs after A23187-induced disruption. This corroborates the findings of others in T84 cells (Tang et al., 2023) as well as in Caco-2 cells (Fernández-Lainez et al., 2023). A fine balance among TJs is required for maintaining paracellular integrity (Chelakkot et al., 2018). Upregulation of specific TJ implies imbalances in TJs and can cause intestinal disorders such as inflammatory bowel disease (IBD) (Fernández-Lainez et al., 2023). A positive observation is that the A23187-induced upregulation of TJs in T84 cells was partly or completely prevented by the presence of SH-SY5Y nerve cells. This attenuation was nerve cell concentration-dependent and particularly strong for *CLDN1* and *CLDN4*. This can be explained by the enhanced expression of *VIP* and *NPY* in the co-cultures. *VIP* and *NPY* have been shown to exert beneficial effects on the gut barrier, as has been extensively described elsewhere (Chandrasekharan et al., 2013). However, the immunofluorescence staining showed higher claudin-1 protein expression when the number of nerve cells increased in A23187-exposed co-cultures. Enhanced claudin 1 protein expression contributes to intestinal integrity (Zhou et al., 2015). This can be partially explained by the concomitant increase in VIP protein expression. However, it could also be partially explained by the fact that despite the inhibition of *CLDN1* gene overexpression by nerve cells to maintain TJ homeostasis, the degradation mechanism of claudin 1 protein is restricted, resulting in protein accumulation during the 24 h of A23187 stimulation.

However, the exact mechanism remains to be further investigated.

HMOs recently gained attention for their health benefits such as supporting gut microbiota colonization and supporting the development of the gut barrier and immune system (Chen and de Vos, 2023). Some hMOs such as 2′-FL have been introduced to the market and are applied in infant formula (Liu et al., 2023). The hMO 3-FL has also been commercially generated and is proposed for health benefits including strengthening of barrier function (Zuurveld et al., 2020). Both 2′-FL and 3-FL have been shown to support the gut mucus layer under homeostasis and allergic conditions (Cheng et al., 2020). Also, 3-FL has been shown to facilitate the development of the epithelial glycocalyx which contributes to microbial colonization in the gut (Kong et al., 2019). However, the effect of hMOs on the interplay between the intestinal epithelium and nerve cells was not explored yet.

Pre-incubation with 2′-FL and 3-FL in T84 cells both significantly attenuated A23187-induced TEER decline, demonstrating their protective effect against intestinal barrier disruption. Our results were in line with previous studies. It found that 2′-FL prevented A23187-induced damage to T84 epithelial cells (Figueroa-Lozano et al., 2021). Pretreatment of Caco-2 cells with 3-FL followed by exposure to IL-6 enhanced TEER and reduced intestinal permeability (Kim et al., 2023). Some hMOs can stimulate Toll-like receptors (TLRs). 2′-FL and 3-FL have been reported to activate TLR-5 and TLR-2, respectively, and both TLR-5 and TLR-2 are involved in the enhancement of TEER and maintenance of intestinal permeability (Figueroa-Lozano et al., 2021). Interestingly, this protective effect of both hMOs on A23187-induced disruption was virtually absent in the presence of nerve cells while in cultures of T84-cells only we found that 2′-FL and to a stronger extent 3-FL rescued epithelial cell barrier function. The hMOs rescued A23187-induced disruption to the same extend as nerve cells. This observation requires some further consideration as in some conditions nerve cell function might be disturbed and substituted by hMOs. This might for example be applicable to individuals with IBD in which structural ENS abnormalities including neuronal cell death have been reported (Lakhan and Kirchgessner, 2010). The hMOs 2′-FL and 3-FL might under these conditions be a substitute for the lower nerve cell numbers and strengthen the intestinal barrier and improve intestinal health.

2′-FL and 3-FL show different patterns of regulation of TJ gene and protein expression in T84 cells and co-cultures. As for TJ gene expression, 2′-FL always prevented A23187-induced upregulation of TJs, especially in the co-cultures of T84:SHSY5Y = 14:1. 3-FL consistently promoted A23187-induced overexpression of *CLDN3* and *ZO-1* in T84 cells, whereas, in the presence of nerve cells, this promotion decreased or was not significant. In TJ protein expression of T84 cells and co-cultures, 3-FL also always showed a greater potency to promote claudin-1 expression than 2′-FL. The difference in impact should be explained by the activation of different sets of receptors by 2′-FL and 3-FL. The hMO 2′-FL is considered to mainly bind to galectin-1, -3, -7, and -9 while 3-FL does not or has a very low binding affinity for these receptors (Shams-Ud-Doha et al., 2017; Zuurveld et al., 2020). Also, hMOs can activate TLR-2 and different patterns of binding to TLR-2 have been demonstrated for the two studied hMOs (Figueroa-Lozano et al., 2021). TLR-2 enhances some TJ such as *ZO-1* through the PKC pathway (Cario et al., 2004). However, based on the previous discussion, we suggest that SH-SY5Y cells stimulated by A23187 inhibited PKC pathways in the gut epithelial cells thereby enhancing TEER. As the number of nerve cells increases, the TLR-2 activated by hMOs may not enhance TJs because of the PKC pathway blocking. Therefore, 2′-FL inhibits more TJs' overexpression induced by A23187 as well as 3-FL progressively reduces A23187-induced overexpression to maintain intestinal TJ expression homeostasis.

In conclusion, our study demonstrates that nerve cells exert a protective effect on A23187-induced disruption of the intestinal epithelial barrier and that this protective effect is nerve cell concentration-dependent. Although hMOs such as 2′-FL and 3-FL do not have any further rescuing effects in the presence of nerve cells, we do demonstrate that in the absence of nerve cells these hMOs can substitute the rescuing effects of nerve cells. As nerve cells can be reduced during intestinal disorders such as IBD, the intake of hMOs may be an effective strategy to enhance intestinal barrier function under these conditions. These findings provide valuable insights into potential therapeutic strategies for maintaining intestinal barrier integrity in IBD. Other strategies may be by enhancing neural growth and function in the intestine as we clearly show the profound effects of nerve cells in rescuing gut epithelial barrier function.

CRediT authorship contribution statement

Xiaochen Chen: Conceptualization, Investigation, Methodology, Validation, Writing – original draft, Writing – review & editing. **Naschla Gasaly:** Investigation, Validation, Writing – review & editing. **Xin Tang:** Investigation, Writing – review & editing. **Marthe T.C. Walvoort:** Resources, Project administration, Supervision, Writing – review & editing. **Paul de Vos:** Funding acquisition, Resources, Project administration, Supervision, Writing – review & editing.

Declaration of competing interest

The authors declare that they have no known competing financial interests or personal relationships that could have appeared to influence the work reported in this paper.

Data availability

Data will be made available on request.

Acknowledgments

This work was supported by a grant from the China Scholarship Council (CSC) to Xiaochen Chen (202107720002). The authors thank **Yang Luo** and **Amalia Dolga** from the Department of Molecular Pharmacology of the University of Groningen for kindly providing the SH-SY5Y cells.

Appendix A. Supplementary data

Supplementary data to this article can be found online at https://doi.org/10.1016/j.crfs.2024.100851.

References

Ali, A., Tan, H., Kaiko, G.E., 2020. Role of the intestinal epithelium and its interaction with the microbiota in food allergy. Front. Immunol. 11, 604054.

Bilginer Kartal, R., Arslan Yildiz, A., 2024. Exploring neuronal differentiation profiles in SH-SY5Y cells through magnetic levitation analysis. ACS Omega 9, 14955–14962.

Cario, E., Gerken, G., Podolsky, D.K., 2004. Toll-like receptor 2 enhances ZO-1-associated intestinal epithelial barrier integrity via protein kinase C. Gastroenterology 127, 224–238.

Chandrasekharan, B., Nezami, B.G., Srinivasan, S., 2013. Emerging neuropeptide targets in inflammation: NPY and VIP. Am. J. Physiol. Liver Physiol. 304, G949–G957.

Chelakkot, C., Ghim, J., Ryu, S.H., 2018. Mechanisms regulating intestinal barrier integrity and its pathological implications. Exp. Mol. Med. 50, 1–9. https://doi.org/10.1038/s12276-018-0126-x.

Chen, X., de Vos, P., 2023. Structure-function relationship and impact on the gut-immune barrier function of non-digestible carbohydrates and human milk oligosaccharides applicable for infant formula. Crit. Rev. Food Sci. Nutr. 1–21.

Cheng, L., Kong, C., Walvoort, M.T.C., Faas, M.M., de Vos, P., 2020. Human milk oligosaccharides differently modulate goblet cells under homeostatic, proinflammatory conditions and ER stress. Mol. Nutr. Food Res. 64, 1900976 https://doi.org/10.1002/mnfr.201900976.

Dai, C.-L., Shi, J., Chen, Y., Iqbal, K., Liu, F., Gong, C.-X., 2013. Inhibition of protein synthesis alters protein degradation through activation of protein kinase B (AKT). J. Biol. Chem. 288, 23875–23883.

di Vito, R., Conte, C., Traina, G., 2022. A multi-strain probiotic formulation improves intestinal barrier function by the modulation of tight and adherent junction proteins. Cells 11, 2617.

Dravid, A., Raos, B., Svirskis, D., O'Carroll, S.J., 2021. Optimised techniques for high-throughput screening of differentiated SH-SY5Y cells and application for neurite outgrowth assays. Sci. Rep. 11, 23935.
Fernández-Lainez, C., aan de Stegge, M., Silva-Lagos, L.A., López-Velázquez, G., de Vos, P., 2023. β (2→ 1)-β (2→ 6) and β (2→ 1) fructans protect from impairment of intestinal tight junction's gene expression and attenuate human dendritic cell responses in a fructan-dependent fashion. Carbohydr. Polym. 320, 121259.
Figueroa-Lozano, S., Akkerman, R., Beukema, M., van Leeuwen, S.S., Dijkhuizen, L., de Vos, P., 2021. 2′-Fucosyllactose impacts the expression of mucus-related genes in goblet cells and maintains barrier function of gut epithelial cells. J. Funct.Foods 85, 104630.
Fleming, M.A., Ehsan, L., Moore, S.R., Levin, D.E., 2020. The enteric nervous system and its emerging role as a therapeutic target. Gastroenterol. Res. Pract. 2020.
Gieryńska, M., Szulc-Dąbrowska, L., Struzik, J., Mielcarska, M.B., Gregorczyk-Zboroch, K.P., 2022. Integrity of the intestinal barrier: the involvement of epithelial cells and microbiota—a mutual relationship. Animals 12, 145.
Kaminsky, L.W., Al-Sadi, R., Ma, T.Y., 2021. IL-1β and the intestinal epithelial tight junction barrier. Front. Immunol. 12, 767456.
Kim, Y.-J., Kim, H.-H., Shin, C.-S., Yoon, J.-W., Jeon, S.-M., Song, Y.-H., Kim, K.-Y., Kim, K., 2023. 2′-Fucosyllactose and 3-fucosyllactose alleviates interleukin-6-induced barrier dysfunction and dextran sodium sulfate-induced colitis by improving intestinal barrier function and modulating the intestinal microbiome. Nutrients 15, 1845.
Kong, C., Cheng, L., Krenning, G., Fledderus, J., de Haan, B.J., Walvoort, M.T.C., de Vos, P., 2020. Human milk oligosaccharides mediate the crosstalk between intestinal epithelial caco-2 cells and lactobacillus plantarum WCFS1in an I n vitro model with intestinal peristaltic shear force. J. Nutr. 150, 2077–2088.
Kong, C., Elderman, M., Cheng, L., de Haan, B.J., Nauta, A., de Vos, P., 2019. Modulation of intestinal epithelial glycocalyx development by human milk oligosaccharides and non-digestible carbohydrates. Mol. Nutr. Food Res. 63, 1900303 https://doi.org/10.1002/mnfr.201900303.
König, J., Wells, J., Cani, P.D., García-Ródenas, C.L., MacDonald, T., Mercenier, A., Whyte, J., Troost, F., Brummer, R.J., 2016. Human intestinal barrier function in health and disease. Clin. Transl. Gastroenterol. 7, e196. https://doi.org/10.1038/ctg.2016.54.
Lakhan, S.E., Kirchgessner, A., 2010. Neuroinflammation in inflammatory bowel disease. J. Neuroinflammation 7, 1–12.
Lee, B., Moon, K.M., Kim, C.Y., 2018. Tight junction in the intestinal epithelium: its association with diseases and regulation by phytochemicals. J. Immunol. Res. 2018 https://doi.org/10.1155/2018/2645465.
Liu, F., van der Molen, J., Kuipers, F., van Leeuwen, S.S., 2023. Quantitation of bioactive components in infant formulas: milk oligosaccharides, sialic acids and corticosteroids. Food Res. Int. 174, 113589.
Liu, S., 2018. Neurotrophic factors in enteric physiology and pathophysiology. Neuro Gastroenterol. Motil. 30, e13446.
Neunlist, M., Toumi, F., Oreschkova, T., Denis, M., Leborgne, J., Laboisse, C.L., Galmiche, J.-P., Jarry, A., 2003. Human ENS regulates the intestinal epithelial barrier permeability and a tight junction-associated protein ZO-1 via VIPergic pathways. Am. J. Physiol. Liver Physiol. 285, G1028–G1036.
Neunlist, M., Van Landeghem, L., Bourreille, A., Savidge, T., 2008. Neuro-glial crosstalk in inflammatory bowel disease. J. Intern. Med. 263, 577–583.
Satsu, H., Yokoyama, T., Ogawa, N., Fujiwara-Hatano, Y., Shimizu, M., 2003. Effect of neuronal PC12 cells on the functional properties of intestinal epithelial Caco-2 cells. Biosci. Biotechnol. Biochem. 67, 1312–1318.
Satsu, H., Yokoyama, T., Ogawa, N., Fujiwara-Hatano, Y., Shimizu, M., 2001. The changes in the neuronal PC12 and the intestinal epithelial Caco-2 cells during the coculture. The functional analysis using an in vitro coculture system. Cytotechnology 35, 73–79.
Shams-Ud-Doha, K., Kitova, E.N., Kitov, P.I., St-Pierre, Y., Klassen, J.S., 2017. Human milk oligosaccharide specificities of human galectins. Comparison of electrospray ionization mass spectrometry and glycan microarray screening results. Anal. Chem. 89, 4914–4921.
Sharkey, K.A., Mawe, G.M., 2023. The enteric nervous system. Physiol. Rev. 103, 1487–1564.
Singh, A., 2023. Brain-derived neurotrophic factor–a key player in the gastrointestinal system. Gastroenterol. Rev. Gastroenterol. 18.
Suzuki, T., 2020. Regulation of the intestinal barrier by nutrients: the role of tight junctions. Anim. Sci. J. 91, e13357.
Takiishi, T., Fenero, C.I.M., Câmara, N.O.S., 2017. Intestinal barrier and gut microbiota: shaping our immune responses throughout life. Tissue Barriers 5, e1373208. https://doi.org/10.1080/21688370.2017.1373208.
Tang, X., Beukema, M., Ferrari, M., Walvoort, M.T.C., de Haan, B.J., de Vos, P., 2023. Efficacy of pectins with different degree of methyl-esterification and of blockiness on preventing gut epithelial cell barrier disruption and impact on sodium-glucose co-transporter expression under low and high glucose conditions. Food Funct.
Walsh, K.T., Zemper, A.E., 2019. The enteric nervous system for epithelial researchers: basic anatomy, techniques, and interactions with the epithelium. Cell. Mol. Gastroenterol. Hepatol. 8, 369–378.
You, X.-Y., Zhang, H.-Y., Han, X., Wang, F., Zhuang, P., Zhang, Y.-J., 2021. Intestinal mucosal barrier is regulated by intestinal tract neuro-immune interplay. Front. Pharmacol. 12, 659716.
Zhou, Q., Costinean, S., Croce, C.M., Brasier, A.R., Merwat, S., Larson, S.A., Basra, S., Verne, G.N., 2015. MicroRNA 29 targets nuclear factor-κB–repressing factor and Claudin 1 to increase intestinal permeability. Gastroenterology 148, 158–169.
Zuurveld, M., Van Witzenburg, N.P., Garssen, J., Folkerts, G., Stahl, B., Van't Land, B., Willemsen, L.E.M., 2020. Immunomodulation by human milk oligosaccharides: the potential role in prevention of allergic diseases. Front. Immunol. 11, 801. https://doi.org/10.3389/fimmu.2020.00801.